Performance of Gamma Stirling Refrigerator having Shell and Tube Condenser and Evaporator

Eldesouki I. Eid, Reda A. Khalaf-Allah, Ahmed M. Soliman, Tamer M. Mansour,Aml A. Mohammed

Abstract— this paper investigates the performance of a gamma-type Stirling refrigerator. The proposed refrigerator has shell and tube condenser and evaporator. In the proposed refrigerator, a wire net regenerator is suggested. The working fluid is selected to be Helium. A drive mechanism controls the synchrony of the reciprocation of both the displacer and the piston. A computer program in the form of a spreadsheet is prepared to solve the refrigerator cycle numerically. The results get the more suitable dimensions of the evaporator, the condenser, the regenerator, the more suitable piston diameter to bore ratio, and the cooling capacity increases continuously with the rotational speed where the COP has a maximum value . The refrigerator develops 0.011596 TR/cc, COP = 0.5597, at 600 rpm and p = 2 bar. The comparison among the present work and previous ones shows that; the present refrigerator explores an enhancement in COP up to 100%, especially at low-speed levels.

Index Terms— Gamma Stirling refrigerator, shell and tube evaporator condenser.

1 Introduction

The Stirling cycle refrigeration is a member of a family of closed-cycle regenerative thermal machines, including prime movers, known collectively as Stirling cycle machines.
Stirling cycle have a good potential for using in the future because of some advantages like external combustion, fuel flexibility and capability to work in the reverse cycle for refrigeration operating.
The traditional working fluids in the Stirling refrigerator are helium, air and carbon dioxide. Despite of many conventional refrigerants these fluids are not harmful to the environment.
Stirling refrigerator and cryocooler have been investigated by many researchers, A. Batooei et al, (2018) explained optimization of a Gamma type Stirling refrigerator is was carried out based on the experimental and analytical results. The cooling capacity and the coefficient of performance (COP) are experimentally was investigated for helium and air. The experimental and simulation results showed that the cooling capacity increases continuously with the rotational speed where the COP has a maximum value. The optimum COP value for helium occurs at higher rotational speed than that of the air. Three parameters namely COP, cooling capacity and pressure drop are investigated in this optimization study. Only helium and carbon dioxide are considered for optimization because of their higher specific heat capacity and enthalpy with respect to air.
N. Parlak et al, (2009) studied a thermodynamic analysis of a gamma type Stirling engine was performed by use a quasi-steady flow model based on Uriel and Berchowitz's works. The Stirling engine analysis was performed for five principal fields: compression room, expansion room, cooler, heater and regenerator. The conservation law of the mass and the energy equations are derived for the related sections. A FORTRAN code is developed to solve the derived equations for all process parameters like pressure, temperature, mass flow, dissipation and convection losses for the different spaces (compression space, cooler, regenerator, heater and expansion space) as a function of the crank angle. The developed model gave more precise results for the pressure profile than the models available in the literature.
S. Alfarawi et al, (2016) was an enhanced thermodynamic model for Gamma-type Stirling engine simulation was developed based on the reconfiguration of non-ideal adiabatic analysis. The developed model was validated against experimental measurements on Stirling engine prototype (ST05 CNC), available at University of Birmingham. Good agreement was found between the model and experiment in predicting the indicated power, shaft power and thermal efficiency at different operating conditions. A parametric study was carried out to investigate the effect of phase angle, gas type, regenerator matrix type and dead volume on engine performance. The feasibility of utilizing the stored cold energy of LN2 to maximize the shaft power was also presented. Results showed that shaft power can be significantly enhanced by 49% for helium and 35% for nitrogen when cooling temperature is lowered to -50 °C while heating temperature remains constant at650 °C.
M. Hooshang et al, (2016) studied a dynamic model of a gamma-type Stirling engine and was examines variations of the crank rotational speed against time (Dynamic response). Kinematic relations of the engine linkages were determined and Lagrange formulations were formed for rigid body dynamics. Working gas pressures on each surface of the rigid bodies were calculated over time using a third order thermodynamic analysis code. A test setup was established for measuring dynamic and thermodynamic state variables of ST500engine. First, experiment data was used to validate the thermodynamic code results. Then the dynamic formulations combined with the thermodynamic code were simultaneously solved and the result is compared to ST500 dynamic response.

Finally, using the whole dynamic model, new aspects of Stirling engine behavior were investigated. The dynamic thermodynamic combination of the model gives the opportunity to instantly calculate a precise open-loop response, which is the essential part of designing proper load controllers for inherently unstable Stirling engines.

M.T. Mabrouk et al, (2014) an analytical model has been developed to evaluate "displacer gap losses" in the clearance between the displacer and the cylinder in both b and g configurations of Stirling engines. Displacer gap losses are the sum of the "shuttle heat transfer" and the "enthalpy pumping". The model was takes into account the pressure gradient in the gap, the gas compressibility and real gas effect. Gas velocity and temperature distributions in the displacer, in the gap and in the cylinder were determined by solving momentum and energy balances in concentric tubes geometry. Our model was then introduced in a whole engine model and the effect of the clearance thickness and engine's speed on total displacer gap losses are investigated.

H. Hachem et al, (2015) a numerical model was developed to optimize a kinematic Gamma Stirling engine. In this model thermal and mechanical loss was included to approximate experimental results. The influences of three operation parameters (filling pressure (3, 5, 10 bar), hot end temperature (300, 400, 500°C) and rotation speed (160, 360, 600 rpm)) as well as heat exchangers efficiencies on the Stirling engine performances was studied. The studied parameters are dependent and their interactions are significant for the Stirling engine brake power. For high initial filling pressure, the brake power became more sensitive to the rotation speed and the hot end temperature. It was found that the performances of the engine are more sensitive to its regenerator efficiency. For $\varepsilon_r = 0.5$ the output brake power and the Carnot efficiency were dropped respectively of 16% and 5% relatively to $\varepsilon_r = 1$.

R. Gheith et al, (2015) studied an optimization of the Stirling engine regenerator's. Firstly, different materials were experimented (Stainless Steel, Copper, aluminum and Monel 400). The engine performances and the state of each material after 15 h of use were considered. The Stainless steel was the material that best satisfies these two conditions. Five regenerators in stainless steel with different porosities were manufactured and experimented (95%, 90%, 85%, 80% and 75%). Porosity that gives the best trade-off between maximizing the engine brake power, maximizing the heat transfer and minimizing the pressure drops, was retained. Thus, the regenerator in stainless steel with porosity of 85% was considered as the most suitable matrix maximizing the Stirling engine performances and minimizing heat and friction losses.

Jizhou He et al, (2002) studied the influence of quantum degeneracy on the performance of a Stirling refrigeration cycle is investigated based on the equation of state of an ideal Fermi gas. The inherent regenerative losses and the coefficient of performance (COP) of the cycle were calculated. It was found that, under the condition of strong gas degeneracy, the COP of the cycle in the first approximation is a function only of the temperatures of the heat reservoirs, while under other conditions; the COPs of the cycle depend on the temperatures of the heat reservoirs and other parameters of the cycle. The results obtained here reveal the general performance characteristics of a Stirling refrigeration cycle having a Fermi gas as its working substance.

E. Luo et al, (2006) introduces a helium-based thermo acoustic refrigeration system, which is a thermo acoustic-Stirling refrigerator driven by a thermo acoustic-Stirling heat engine, for domestic refrigeration purpose. In the regenerators of both the refrigerator and the prime mover, helium gas experiences near to reversible high efficiency Stirling process. At the operating point with 3.0 MPa mean pressure, 57.7 Hz frequency, and 2.2 kW heat input, the experimental cooler provides a lowest temperature of −64.4 °C and 250 W cooling power at −22.1 °C. These results show good potential of the system to be an alternative in near future for domestic refrigeration with advantages of environment-friendliness, no moving parts, and heat driven mechanism.

Q. Zhou et al, (2015) Showed experimental results of cryogenic regenerator materials employed in Stirling-type one-stage pulse-tube refrigerator for the use at liquid hydrogen temperature. Thermal diffusion coefficients, the suitable regenerator materials, prove to be a usefully reference. Discuss the impact of resistance of sphere regenerator materials on the performance of the refrigerator and the method to improve it. Was Take an overall consideration, was suitable-size Er3Ni will be applied as the regenerator materials at the cold head and we achieve a remarkable 14.7 K no-load temperature.

H. Karabulut et al, (2006) studied how reduce the external volume of Stirling engines and to increase the specific power per unit volume, a novel mechanical arrangement is used where the power cylinder is concentrically situated inside the displacer cylinder. The inner heat transfer surface requirement and the thermodynamic performance characteristics are predicted preparing a nodal analysis in FORTRAN, The analysis indicates that the heats received from and delivered to the regenerator are not equal to each other. Therefore, the ends of the regenerator should be coupled with a heater and a cooler. The maximum thermal efficiency appears at the minimum mass of working fluid as the minimum thermal efficiency appears at the maximum mass of working fluid. The work increases up to a certain value of working fluid and then decreases. The thermal efficiency increases until a certain value of regenerator area and then decreases as well. Fluid temperature in the hot volume and cooler differs from the wall temperature at significant rates.

Carl E Mungan, (2017) in this article Stirling refrigerator configurations analyzed at a level of presentation suitable for thermodynamics. Explained that coefficient of performance depends on whether the non-isothermal heat exchanges were performed reversibly or if the working fluid was an ideal gas. The theoretical performance of the fridge can then attain the reversible Carnot limit if a regenerator was used, which is a high heat capacity material through which the gas flows. N. SOREA et al, (2009) presents a computer simulation of

Gamma Stirling engine in Gamma Stirling Engine Simulator software and studied the influence of the phase angle on the operating characteristics.

Kai Wang et al, (2016) presents for the research development of Stirling cycle engines for recovering low and moderate temperature heat. . Upon comparing the available experimental results and the technology potentials, concluded that kinetic Stirling engines and thermo acoustic engines have the greatest application prospect in low and moderate temperature heat recoveries in terms of output power scale, conversion efficiency, and costs. that a cost effective Stirling cycle engine was practical for recovering small-scale distributed low-grade thermal energy from various sources.

W.Lih Chen et al,(2014) Submitted the studied some important information for the design of moving regenerator in a gamma-type Stirling engine where been studied a helium charge gamma-type twin power piston Stirling engine experimentally to understand the effects of several regenerator parameters on the overall performance of the engine. Stacked-woven metal screens have been used as regenerator matrix materials. The results include engine shaft torque, power, and efficiency versus engine speed at several engine's hot-end temperatures. It is found that all parameters pose significant impact on engine performance and as well as regenerator matrix screens have to be installed in a manner that the working-gas-flow direction is normal to the surface of matrix screens; very small wire diameter results in large pressure drop and reduce regenerator effectiveness; and there exists an optimal fill factor.

A. Ashok et al, (2015) the gamma type is very economical and simple in fabrication. Has designed and fabricated a Gamma-type Stirling engine with rotary displacer for utilizing the waste heat in a cost for a better economy. Designed the engine to utilize the waste heat from the steam-boiler. This simple Engine can be easily fabricated and can be used for house-hold applications.

R. Gheith et al, (2011) present the measurement and performance of a gamma Stirling engine of 500W of mechanical shaft power and 600 rpm of maximal revolutions per minute. Series of measurements concerning the pressure distribution, temperature evolution, and brake power were performed. The working fluid temperature measurements have been recorded in different locations symmetrically along both regenerator sides. The recorded temperature in regenerator side one is about 252 °C and about 174 °C in the opposite side (side two). It shows an asymmetric temperature distribution in the Stirling engine regenerator; consequently, heat transfer inside this porous medium is deteriorated.

S. Banerjee et al, (2016) the performance parameters of a gamma type Low Temperature Differential Stirling engine was studied under the effect of different cooling mediums. The cold end of the displacer cylinder of the Stirling engine was provided with a cooling chamber through which the coolants were pumped and circulated continuously. The performance characteristics were tested for three different coolants. Simple water, ethylene Glycol based coolant and propylene glycol based coolant. The maximum torque observed is 1.42 Nm at 110 rpm for ethylene glycol based coolant and maximum shaft power observed was 28.1658 W at 234 rpm for propylene glycol based coolant.

K.Effah et al, (2017) studied use a third order quasi-steady flow model to predict the performance of an experimental gamma type Stirling engine at the heater temperature of 1145K by simulating in MATLAB environment. A prediction error of 8.24% was obtained after comparing simulated performance with the experimental values. Empirical methods such as Beale and West analysis were also used to predict the performance of the Stirling engine. The quasi-steady flow model showed better accuracy when compared to other methods such as Beal and West analysis.

R. Gheith et al, (2012) a gamma Stirling engine with compressed air as working fluid was investigated. Four different materials were investigated: stainless steel, copper, aluminum and Monel 400. The obtained experimental results provide guidance to Stirling engine enhancement and selection of the appropriate regenerator material. the regenerator has an important role to enhance the heat exchange and to improve Stirling engine performance, which closely depends on its constituting material ,the stainless steel regenerators for an acceptable thermal efficiency and do not oxidize.

H. El Hassani et al, (2014) studied experimentally and theoretically the effect of some geometrical parameters on low temperature differential Stirling engines (LT-SE) performance. The studied parameters are: the phase angle, the compression ratio and the dead volume. Results show that for optimizing the performance of these engines, dead volume should be minimized, the compression ratio should be maximized and the optimal phase angle for the gamma type is 90°.

R.K. Bumataria et al, (2013) submitted a new and complete model for a Stirling engine has been established. This computerized model predicts the behavior of existing engines reasonably accurately for cases where a quantitative comparison is available. In order to obtain a closed solution suitable for design optimization a simplified model for a Stirling engine has been derived considering different types of losses in this engine. This new model has sufficient accuracy for prediction of the behavior a real engine and its results are quite close to the complete model predictions.

J. ZARINCHANG et al, (2008) the heat exchangers are the most important parts of Stirling engine. These heat exchangers are Heater, Regenerator and Cooler which exchange heat to and from the engine. The design and configuration of these heat exchangers effect on engine performance. The optimization of these parts for a 20 kW Stirling engine is was shown.

T. Otaka et al, (2002) provided a theoretical investigation on the thermodynamic analysis of a Stirling engine with linear and sinusoidal variations of the volume. The regenerator in a Stirling engine is an internal heat exchanger allowing reaching high efficiency. Was show that the engine efficiency with perfect regeneration doesn't depend on the regenerator dead volume but this dead volume strongly amplifies the imperfect regeneration effect. An analytical expression to estimate the improvement due to the regenerator has been proposed in-

cluding the combined effects of dead volume and imperfect regeneration. This could be used at the very preliminary stage of the engine design process.

2. GAMMA – REFRIGERATOR

2.1.Proposed refrigerator

The proposed Gamma-refrigerator shown in Fig. 1 consists of two cylinders having of 100mm bore. The shell and tube heat exchanger of suggested as an evaporator and a condenser. While, a wire mesh suggested being the regenerator. The reciprocation of both displacer and piston controlled by a drive mechanism. Helium selected as working media. The refrigerator has been analyzed in the vision of Schmidt theory, considering the pressure losses through the heat exchanger.

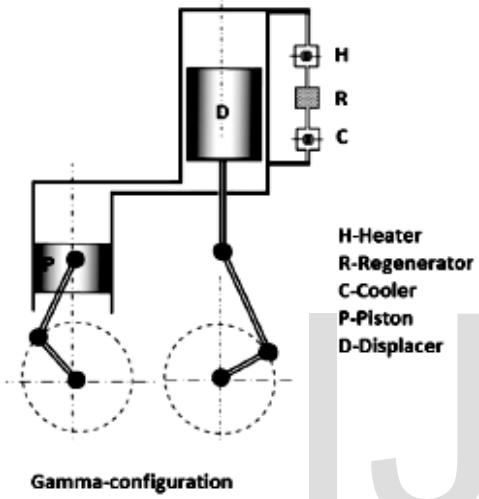

Fig.1. Scheme of the gamma type Stirling refrigerator.

2.2. Schmidt analysis of the refrigerator

Fig. 2 shows the drive mechanism and equivalent volume volumes for each of the compression and expansion spaces are as follows [3],

$$y_p = r_p \sin\Phi + l_p \sin\Phi_1 \quad (1)$$

$$\Phi_1 = \cos^{-1}\left[\frac{-r_p.\cos(\Phi)}{l_p}\right] \quad (2)$$

$$y_d = r_d.\sin(\Phi+\alpha) + l_d.\sin(\Phi_2) \quad (3)$$

$$\Phi_2 = \cos^{-1}\left[\frac{-r_d.\cos(\Phi+\alpha)}{l_d}\right] \quad (4)$$

Fig.3 shows both displacer and piston movements, and therefore, the swept volume of both compression and expansion spaces can express as follows:

$$V_{C1,sw} = \frac{\pi}{4} D_P{}^2 \left(y_{p(max)} - y_{p(\Phi)}\right) \quad (5)$$

$$V_{C2,sw} = \frac{\pi}{4} D_d{}^2 \left(y_{d(\Phi)} - y_{d(min)}\right) \quad (6)$$

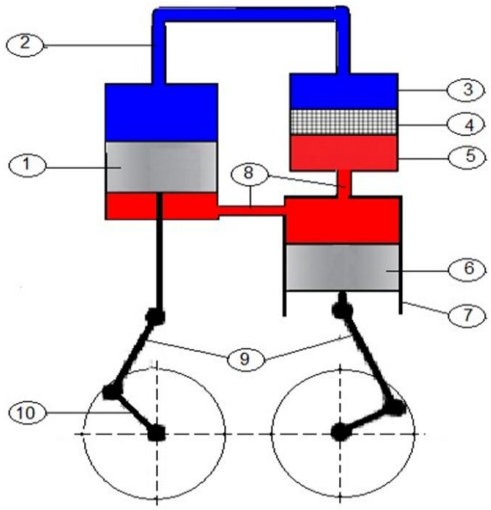

1	Displacer	6	Piston
2	Transport port	7	Cylinder
3	Evaporator	8	Transport port Com-
4	Regenerator	9	Connecting rod
5	Condenser	10	Crank radius

Figure 2. Scheme of the proposed refrigerator.

$$V_{E,sw} = \frac{\pi}{4} D_d{}^2 \left(y_{d(max)} - y_{d(\Phi)}\right) \quad (7)$$

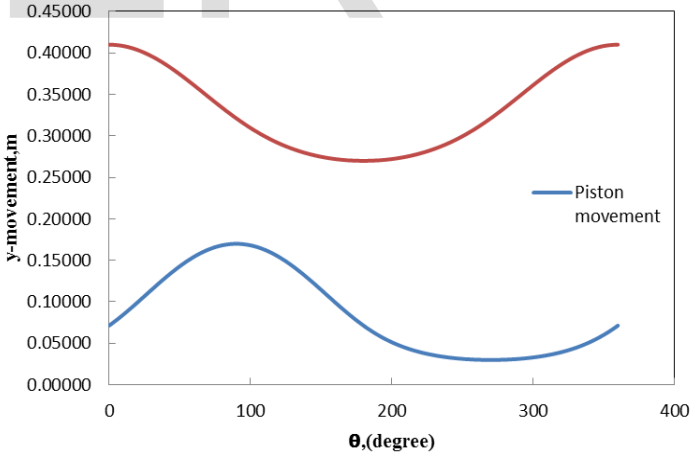

Fig.3. Piston and displacer movement versus crank angle

Fig.4 shows the total volume of the refrigerator workspace is as follows:

$$V_t = V_E + V_{tp,E} + V_s + V_r + V_c + V_{tp,c} + V_C \quad (8)$$

According to Schmidt assumptions, [23], the temperature of the regenerator T_r is:

$$T_r = \frac{T_C - T_E}{\ln \frac{T_C}{T_E}} \quad (9)$$

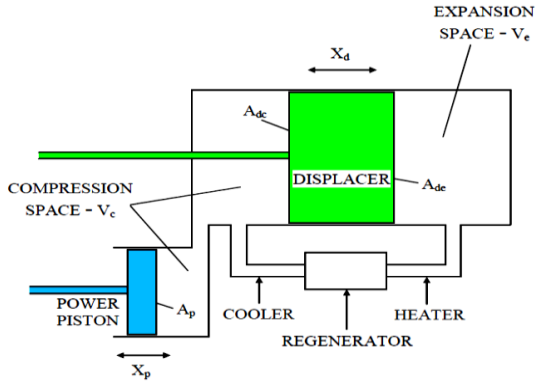

A_{de} = the area of the displacer on the expansion space side	
A_{dc} = the area of the displacer on the compression space side..	
A_p = the area of the power piston	V_e = the volume in the expansion space
X_d = the stroke length of the displacer	V_c = the volume in the compression space
X_p = the stroke length of the power piston	

Fig. 4. Shows both piston and displacer movements.

The total charged mass of the working fluid is:

$$m_t = p\left[\frac{(V_E + V_{tp,E} + V_e)}{R\,T_E} + \frac{V_r}{R\,T_r} + \frac{(V_c + V_{tp,c} + V_C)}{R\,T_C}\right] = \frac{p_{ch} V_{max}}{R T_{ch}} \quad (10)$$

Thus, the instantaneous Schmidt pressure, [1] is:

$$p = \frac{m_t}{\left[\frac{(V_E + V_{tp,E} + V_e)}{R\,T_E} + \frac{V_r}{R\,T_r} + \frac{(V_c + V_{tp,c} + V_C)}{R\,T_C}\right]} \quad (11)$$

Thus, Schmidt p-V diagram is as shown in Fig. 5.

Applying the mass conservation equation among the refrigerator workspaces, the cyclic flow rate through the heat exchangers cleared in Fig. 6. The instantaneous Reynolds numbers are as follows:

$$\left(Re_{tp,c}\right)_{\Phi=n} = \left[\frac{\rho_{tp,c} v_{tp,c} d_{tp,c}}{\mu}\right]_{\Phi=n} \quad (12)$$

$$Re_e = \left[\frac{4\dot{m}}{\pi\, d_h\, \mu}\right]_e \quad (13)$$

$$Re_r = \left[\frac{16\,\dot{m}\,(1-\psi)}{\pi\, d_w\, \mu\, \psi}\right]_r \quad (14)$$

$$Re_c = \left[\frac{4\dot{m}}{\pi\, d_h\, \mu}\right]_c \quad (15)$$

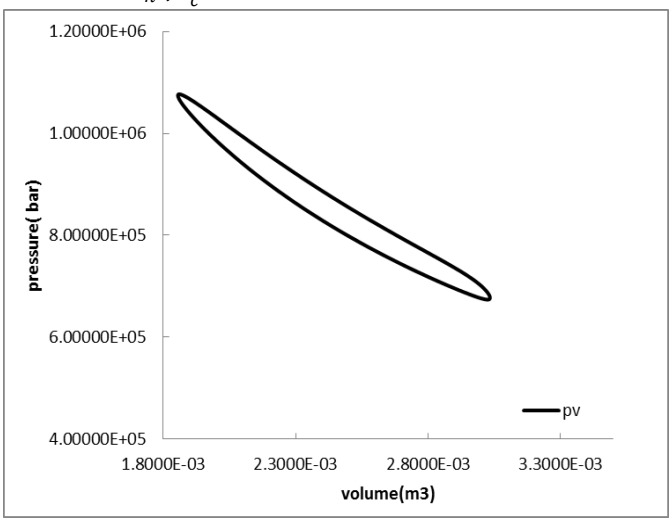

Fig. 5. Schmidt p – V diagram at a charge pressure of 7 bar.

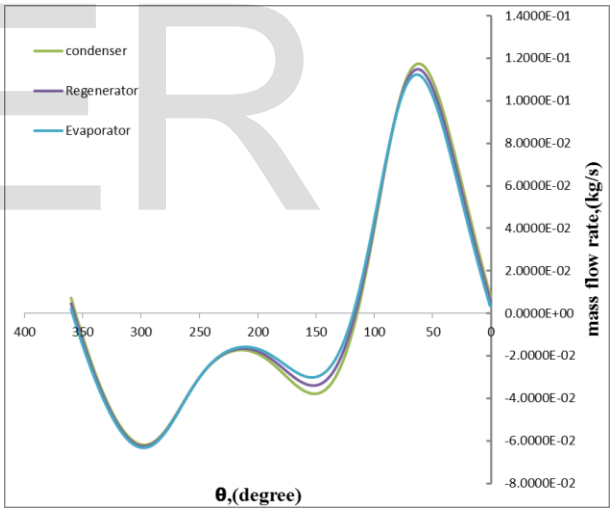

Fig.6. Cyclic mass flow rate through the evaporator, condenser, and the regenerator.

The heat absorbed and rejected rates are as follows, [23]:

$$Q_e = N \oint p_E dV_E \quad (16)$$

$$Q_c = N \oint p_C dV_C \quad (17)$$

From these calculations, can be calculated Nusselt number for the fluid flow inside the tube in the heat exchangers using the correlations in the Ref [36] as shown below, The

Prandtl number and Reynolds number range for these equations are 104<Re < 5 x 106 and 0.5 <Pr < 2000.

For turbulent flow can be used equation (18):

$$Nu = \frac{(f/2).Re.Pr}{1.07 + 12.7(f/2)^{1/2}.(Pr^{2/3} - 1)} \quad (18)$$

For laminar flow, can be used equation (67)

$$Nu = 1.86\left(\frac{d_i.Re.Pr}{L}\right)^{1/3} \quad (19)$$

$$Nu = hd/k \quad (20)$$

$$f = (1.58.\ln Re - 3.28)^{-2} \quad (21)$$

The frictional pressure drop due to the fluctuating flow through the condenser and evaporator the can be determined as follows, [23]:

$$\Delta p = 1.6\left[4\left[\frac{f.L_t}{d_i} + 1\right].N_p.\frac{\rho.v^2}{2}\right] \quad (22)$$

The regenerator is formed of consecutive similar layers of stainless-steel wire net. The pressure drops in the regenerator due to fluctuating flow was determined as follows, [34]:

$$\log(f_R) = 1.73 - 0.93\log(Re_R), if\ 0 < Re_R \le 60 \quad (23)$$

$$\log(f_R) = 0.714 - 0.365\log(Re_R), if\ 60 < Re_R \le 1000 \quad (24)$$

$$\log(f_R) = 0.015 - 0.125\log(Re_R), if\ Re_R > 1000 \quad (25)$$

$$\psi = 1 - \frac{1000i}{25.4} \times \frac{\pi}{4} d_w \quad (26)$$

$$\Delta p_R = f_R.(L_R/d_{hyd}).\rho_R.(v_R^2/2) \quad (27)$$

$$d_{hyd} = d_w\sqrt{\frac{\psi}{1-\psi}} \quad (28)$$

The regenerator effectiveness is:

$$\varepsilon = NTU_R/(1 + NTU_R) \quad (29)$$

$$NTU_R = 2\overline{St_R} \times (L_R/d_{h,R}) \quad (30)$$

$$St_R = 0.595/(Re_R^{0.4}.Pr_R) \quad (31)$$

The P–V diagrams for both compression and expansion spaces considering pressure losses are shown in fig.7. Thus, the coefficient of performance for refrigerator, [12]:

$$COP = Q_e^{\cdot}/(Q_c^{\cdot} - Q_e^{\cdot}) \quad (32)$$

2.3 FLOW CHART AND COMPUTER PROGRAM:

By use the excel computer program in the form of a worksheet to solve the former equations numerically. All parameters were calculated directly with the crank angle. The temperature of the refrigerated space was had constant at -10 ^{0}C. Also, the cooling water temperature was retained constant at 20 ^{0}C. The crank angle changed at 1.0 - degree step. The regenerator effectiveness was kept more than or equal 97%.
The bore fixed at 0.1 m. The outer diameter of the shell equals the bore for the condenser and evaporator. The dimensions of the heat exchangers, number of tubes, phase angle, stroke, charging pressure, and speed was different to get the most proper values that result in higher cooling load and COP. The flow process which highlights the procedure of the numerical calculations that are classified with the previous data is shown in fig.8.

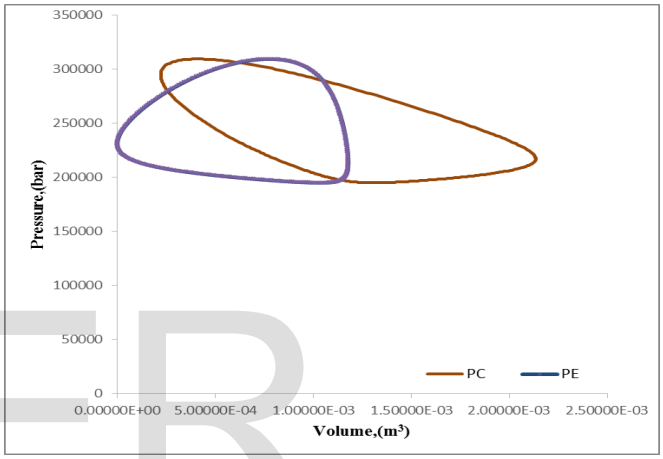

Fig.7. p – V diagrams for both expansion and compression spaces.

2.4 CALCULATED DIMENSIONS OF THE REFRIGERATOR

The more suitable data of the gamma type Stirling refrigerator are as following, in the tble:

Refrigerator	Gamma type
Speed	900 rpm
Charge pressure	2.0 bar
Working fluid	Helium
Compression and Expansion Bore, D	0.1m
Piston stroke	1.5D
Displacer stroke	1.5 D
Evaporator	
Le	0.5 D
de	0.02 D
N	265 tubes
Regenerator	
Lr	0.3 D
dr	D
i	100 pores/inch
Condenser	
Lc	0.6 D
dc	0.025 D
N	265 tubes

INTERNATIONAL JOURNAL OF SCIENTIFIC & ENGINEERING RESEARCH VOLUME 10, ISSUE 3, MARCH-2019
ISSN 2229-5518

3. Results and Discussion

3.1. Effect of the diameter of both condenser and evaporator

Referring to Fig. 9, the increase in evaporator inner diameter decreases Reynolds number also decreases the convective heat transfer coefficient, but the surface area increases which increase the cooling load. The more increase in the evaporator diameter reduces the cooling load due to the more increase in dead space.
The more suitable evaporator inner diameter is around 0.07 D. Also, one can say, the more accepted condenser internal diameter is about 0.04 D, as noted in Fig. 10.

3.2. Effect of the length of both evaporator and condenser

Referring to Fig. 11, a sharp reduction in both cooling load and COP with the rise of the evaporator length observed due to the higher increase in both dead space and pressure losses.
The selected evaporator length to get high cooling load is 0.5 D. Also, the selected condenser length to get high cooling load is 0.6 D, as manifest in Fig. 12.

3.3. Effect of the regenerator dimensions

Referring to Fig.13, the increase in the mesh number reduces the porosity as well as the free flow area which resists the fluctuating of the working fluid, higher-pressure losses, and more required driven power. The more acceptable mesh size is almost 100 pores per inch. Also, the height of the regenerator to get so-called perfect effectiveness is about 0.25 D as clear in Fig. 14.

3.4. Effect of the diameter of piston to displacer (bore) ratio

Referring to Fig. 15, to get 573.44 W cooling loads, which is the maximum allowable value, one can suggest the diameter of piston to displacer (bore) ratio to be about 0.8 D to 1 D. to COP about 0.55 of Carnot COP. The increase in the diameter of piston to displacer (bore) ratio increases the cooling load therefore decrease COP, due to, the increase in the flow velocity through the heat exchangers which increases the pressure drop and consequently an increase of the prime mover power required to drive the refrigerator.

3.5. Effect of the pressure drop and speed

In Fig. 16, the more increase in speed the cooling load increases with low COP. The increase in the speed increases the pressure drop .On the other hand, in fig.17 if the importance factors of COP and cooling capacity are higher than pressure drop, the optimum rotational speed is taken place in the range of 500 rpm to 900 rpm, for helium. If the importance factors of pressure drop and cooling capacity are higher than COP, the optimum point is occurred between 800 rpm to 1000 rpm for helium.

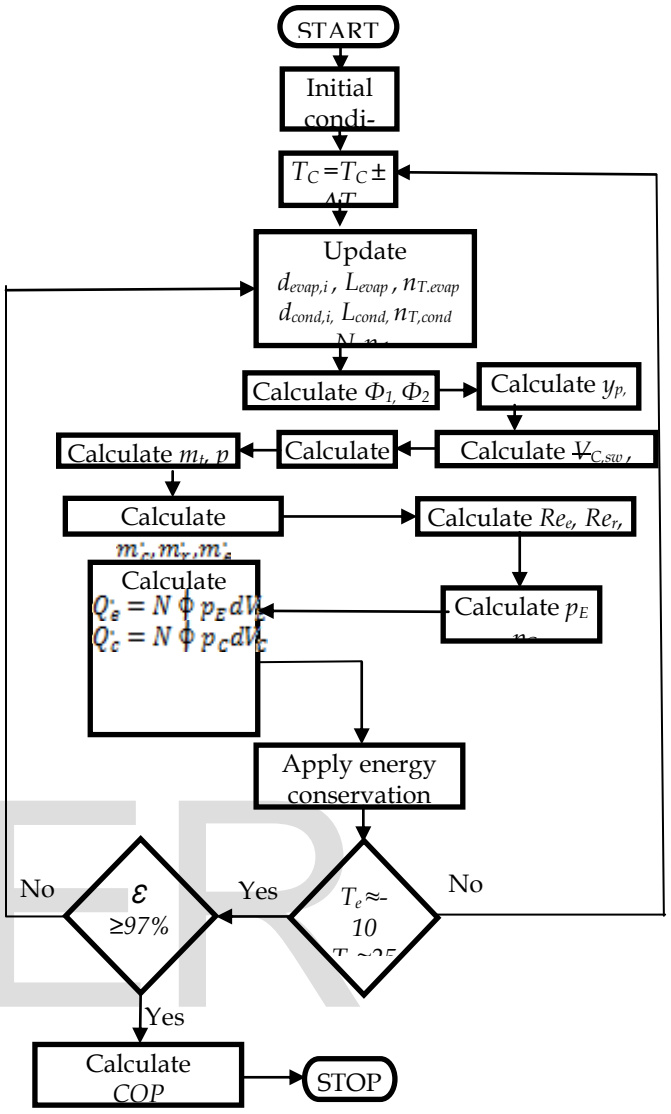

Fig.8. the flow algorithm which highlights the procedure of the numerical calculations.

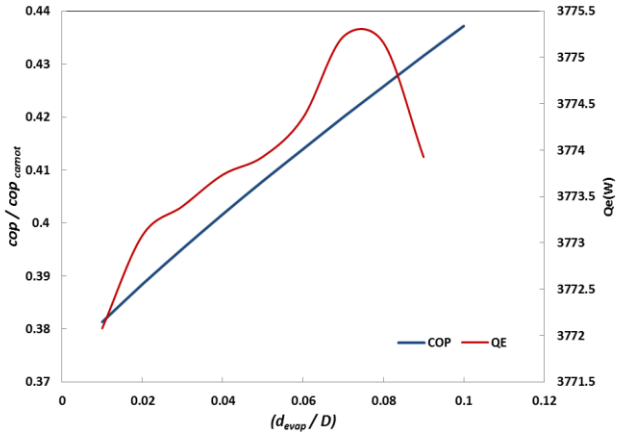

Fig.9. Coolng load and COP versus inner diameter of the evaporator tube.

INTERNATIONAL JOURNAL OF SCIENTIFIC & ENGINEERING RESEARCH VOLUME 10, ISSUE 3, MARCH-2019
ISSN 2229-5518

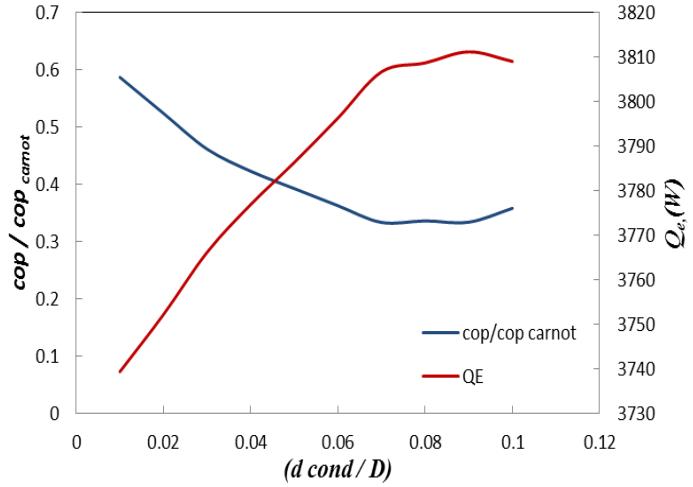

Fig .10. Cooling load and COP versus inner diameter of the condenser tube ratio.

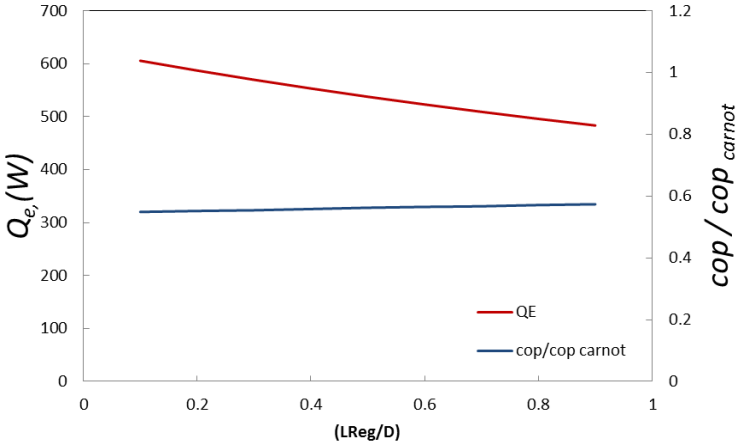

Fig. 14. Cooling load and COP versus the regenerator length.

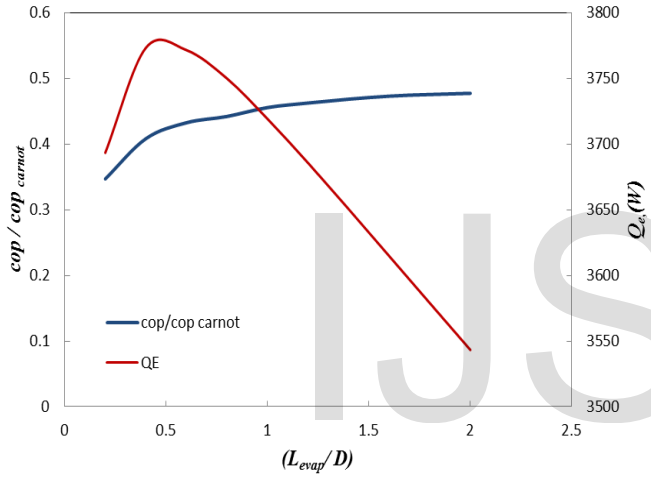

Fig.11. Cooling load and COP versus length of the evaporator tube ratio.

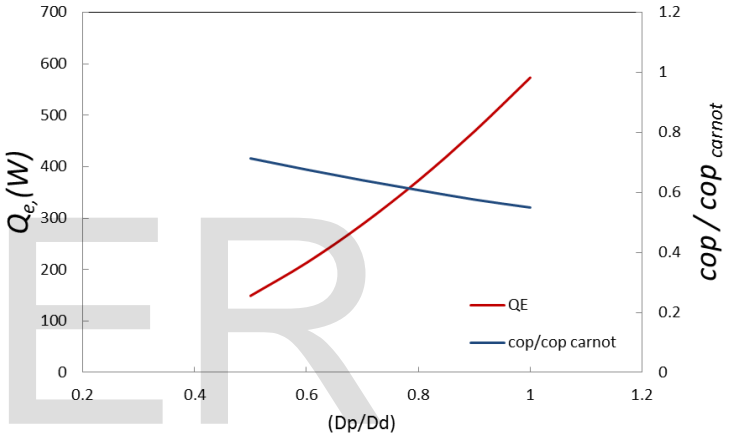

Fig. 15. Effect of the diameter of piston to displacer (bore) ratio.

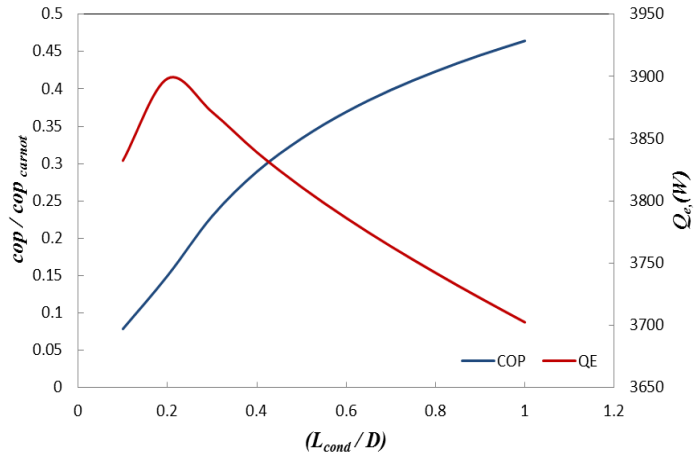

Fig.12. Cooling load and COP versus length of the condenser tube ratio.

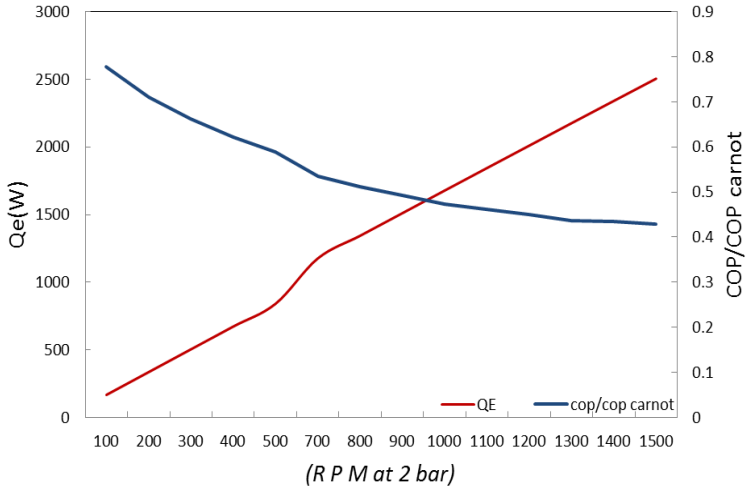

Fig. 16. Cooling load and COP versus the speed.

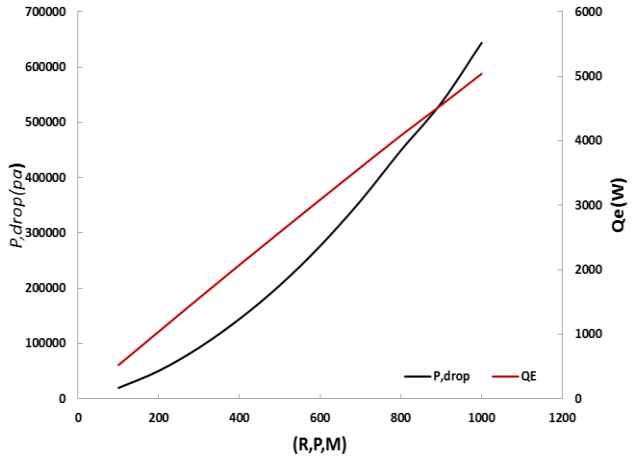

Fig. 17. Cooling load and pressure drop versus the speed.

4. Comparison among the present work and the previousones

The multi-objective optimization of Gamma type Stirling refrigeration using Helium as a working fluid done by Ref. [1]. Fig. 24 shows a so-well-suited and so-acceptable trending among present results and previous ones. The comparison shows that; the suggested refrigerator explores an enhancement in COP up to 100%, especially at low-speed levels.

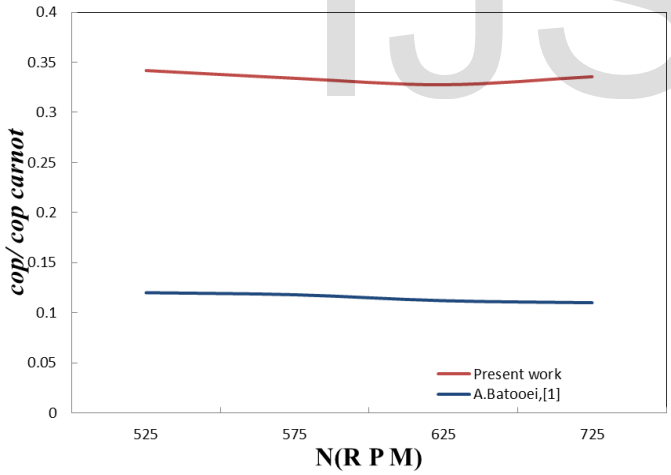

Fig. 18. Comparison among present work and previous ones.

5. Conclusions

The present work deals with the performance of gamma type Stirling refrigerator using shell and tube heat exchange the evaporator and the condenser.The principal dimensions of the refrigerator that result in higher cooling load and better COP found. The study monitored the more acceptable dimensions of the evaporator, regenerator, condenser, and piston diameter. The principal results briefly systemized as the following items:

1- The more acceptable dimensions of the refrigerator to develop higher heat removal rate with a considerable COP were determined.

2- The refrigerator can be manufactured using the calculated dimensions to validate its performance experimentally.

3-The comparison among present results and previous one shows a so-well-suited and so-acceptable trending and shows that the present refrigerator explores an enhancement in COP up to 100%, especially at low-speed levels.

4-The cooling capacity increases continuously with the rotational speed when the helium was used as the working fluid.

5-If the importance factors of COP and cooling capacity are higher than the pressure drop; the optimum point takes place at higher rotational speed

6-The cooling capacity and COP values for both helium increases with the charging pressure.

NOMENCLATURE

Symbols	Description	Unit
A	Surface area	m^2
d	Tube diameter,	m
f	Friction coefficient	
h	Heat transfer coefficient	$Wm^{-2}K^{-1}$
i	Wire mesh number	*pores/inch*
k	Thermal conductivity	$Wm^{-1}k^{-1}$
L	Length	m
l	Connecting rod Length	m
m	Mass	kg
$\dot{m}$	Mass flow rate	kg/s
N	Speed	rpm
n	Number of tubes	
NTU	Number of transfer of units	

Symbols	Description	Unit
p	Pressure	pa
q.	Heat transfer rate	w
r	Specific gas constant	Jkg-1 K-1
r	Crank radius	m
re	Reynolds number	
st	Stanton number	
t	Temperature	K
t	Time	s
v	Volume	m3
v	Velocity	ms-1

Greek Letters

α	Phase angle	Rad
Ɛ	Regenerator effective-	
Φ	Crank angle	radian
Φ1, Φ2	Connecting rod angle	radian
μ	Viscosity	kg m-1s-1
ϱ	Density	kg m-3
Ψ	Porosity	

SUBSCRIPTS

C	Compression space
cl	Clearance
cond	Condenser
Reg	Regeneretor
d	Displacer
E	Expansion space
evap	Evaporator

REFERENCES

[1] A. Batooei, A. Keshavarz, A Gamma type Stirling refrigerator optimization, an experimental and analytical investigation, Int. J. Refrig. 91 (2018) 89-100.

[2] N. Parlak, A. Wagner, et al, Thermodynamic analysis of a gamma type Stirling engine in non-ideal adiabatic conditions, Renewable Energy. 34 (2009) 266–273.

[3] S. Alfarawi, R. AL-Dadah, et al, Enhanced thermodynamic modelling of a gamma-type Stirling engine, Applied Thermal Engineering 106 (2016) 1380–1390.

[4] M. Hooshang, R. Askari Moghadam, et al, Dynamic response simulation and experiment for gamma-type Stirling engine, Renewable Energy 86 (2016) 192-205.

[5] M.T. Mabrouk, A. Kheiri, et al, Displacer gap losses in beta and gamma Stirling engines, Energy xxx (2014) 1-10.

[6] H. Hachem, R.Gheith,et al, Numerical characterization of a c-Stirling engine considering losses and interaction between functioning parameters, Energy Conversion and Management 96 (2015) 532–543.

[7] R. Gheith, F. Aloui, et al, Determination of adequate regenerator for a Gamma-type Stirling engine, Applied Energy 139 (2015) 272–280.

[8] J. He, J. Chen, B. Hua ,Influence of quantum degeneracy on the performance of a Stirling refrigerator working with an ideal Fermi gas, Applied Energy 72 (2002) 541–554.

[9] Y. Zhang, et al, Thermoacoustically driven refrigerator with double Thermoacoustic-Stirling cycles, APPLIED PHYSICS LETTERS 88, 074102 (2006).

[10] Q. Zhou, L. Chen, Ch. Pan, Y. Zhou, J. Wang, Experimental investigation on regenerator materials of Stirling-type pulse-tube refrigerator working at 20 K, Physics Procedia 67 (2015) 530 – 535.

[11] H. Karabulut, H.S. Yucesu, C. Cinar, Nodal analysis of a Stirling engine with concentric piston and displacer, Renewable Energy 31 (2006) 2188–2197.

[12] Carl E Mungan, Coefficient of performance of Stirling Refrigerators, European Journal of Physics38 (2017) 055101 (9pp).

[13] N.SOREA, D. CERNOMAZU, The Phase Angle Influence on the Operating Characteristics of Gamma Stirling Engine, 3rd International Symposium on Electrical Engineering and Energy Converters (2009) 24-25.

[14] K. Wang, S.Sanders, S.Dubey, F.H.Choo, F.Duan, Stirling cycle engines for recovering low and moderate temperature heat: A review, Renewable and Sustainable Energy Reviews 62(2016)89–108.

[15] W.L Chen, K.L. Wong, H.E. Chen, An experimental study on the performance of the moving regenerator for a c-type twin power piston Stirling engine, Energy Conversion and Management 77 (2014) 118–128.

[16] Ashok, Arundas. S, B. Varghese, Ajithkumar.K.T ,DESIGN AND FABRICATION OF GAMMA-TYPE STIRLING ENGINE WITH ROTARY DISPLACER , International Journal of Research in Engineering and Technology 04(2015) eISSN: 2319-1163 | pISSN: 2321-7308.

[17] R.Gheith, F. Aloui, M.Tazerout, and S. B. Nasrallah, Experimental investigations of a gamma Stirling engine, INTERNATIONAL JOURNAL OF ENERGY RESEARCH (2011).

[18] S. Banerjee, K. Ganguly, B. Dewangan, R. Kumar, Performance testing of a gamma type Stirling engine for different cooling mediums, International Journal of Mechanical Engineering Volume 4, Issue 3, (2016).

[19] Kwasi-Effah C. C, Obanor A. I, Aisien F. A, Ogbeide O. O, Performance Appraisal of a Gamma-Type Stirling Engine, International Journal of Oil, Gas and Coal Engineering (2017) 5(4): 51-53.

[20] R.Gheith, F. Aloui, and S.B. Nasrallah, Study of the regenerator constituting material influence on a gamma type Stirling engine, Journal of Mechanical Science and Technology 26 (4) (2012) 1251-1255.

[21] H. El Hassani, N. Boutammacht , M. Hannaoui, Study of Some Power Influencing Parameters of a Solar Low Temperature Stirling Engine, European Journal of Sustainable Development (2014), 3, 2, 109-118.

[22] R. K. Bumataria, N. K. Patel, STIRLING ENGINE PERFORMANCE PREDICTION USING SCHMIDT ANALYSIS BY CONSIDERING DIFFERENT LOSSES, International Journal of Research in Engineering and Technology Volume: 02 Issue: 08 | (2013).

[23] A.A. El-Ehwany, G.M. Hennes, E.I. Eid , E.A. El-Kenany, Development of the performance of an alpha-type heat engine by using elbow-bend transposed-fluids heat exchanger as a heater and a cooler, Energy Conversion and Management 52 (2011) 1010–1019.